

The Role of Type II Spicules in the Upper Solar Atmosphere

J. A. Klimchuk¹

J. A. Klimchuk, Heliophysics Division, NASA Goddard Space Flight Center, 8800 Greenbelt Road, Greenbelt, MD 20771, USA. (James.A.Klimchuk@nasa.gov)

¹Heliophysics Division, NASA Goddard Space Flight Center, Greenbelt, Maryland, USA.

Abstract. We examine the suggestion that most of the hot plasma in the Sun's corona comes from type II spicule material that is heated as it is ejected from the chromosphere. This contrasts with the traditional view that the corona is filled via chromospheric evaporation that results from coronal heating. We explore the observational consequences of a hypothetical spicule dominated corona and conclude from the large discrepancy between predicted and actual observations that only a small fraction of the hot plasma can be supplied by spicules ($<2\%$ in active regions and $<5\%$ in the quiet Sun). The red-blue asymmetries of EUV spectral lines and the ratio of lower transition region (LTR; $T \leq 0.1$ MK) to coronal emission measures are both predicted to be 2 orders of magnitude larger than observed. Furthermore, hot spicule material would cool dramatically by adiabatic expansion as it rises into the corona, so coronal heating would be required to maintain the high temperatures that are seen at all altitudes. The necessity of coronal heating is inescapable. Traditional coronal heating models predict far too little emission from the LTR, and we suggest that this emission comes primarily from the bulk of the spicule material that is heated to ≤ 0.1 MK and is visible in He II (304 \AA) as it falls back to the surface.

1. Introduction

One of the great challenges facing space science has been to explain the million degree plasma observed in the solar corona and the coronae of other late-type stars. The underlying atmosphere is much colder, so the hot plasma cannot be energized by a thermal conduction flux from below. It is generally assumed that some mechanism such as magnetic reconnection or waves heats the plasma locally to high temperatures. This traditional view is now being challenged by new observations. Small finger-like ejections of chromospheric material have been discovered and given the name type II spicules [De Pontieu *et al.*, 2007]. They differ from ordinary spicules in that they are thinner (< 200 km), faster ($50\text{-}150 \text{ km s}^{-1}$), and shorter-lived ($10\text{-}150$ s). Another important property is that a fraction of the cold mass is heated to coronal temperatures as it is ejected (De Pontieu *et al.* [2011]; although see Madjarska, Vanninathan, and Doyle [2011]). This raises the possibility that much or even most of the plasma observed in the corona comes from type II spicules and that heating in the corona itself is unnecessary [De Pontieu *et al.*, 2009, 2011]. The proposal that spicules supply the corona with its mass is not new [Athay and Holzer, 1982], but the idea was largely rejected because ordinary spicules are not observed to reach coronal temperatures. Although it is not universally accepted that type II spicules are different from ordinary spicules [Zhang *et al.*, 2012], the new observations show that at least some hot material is transported to the corona during some ejections.

The primary purpose of this paper is to make an initial assessment of whether type II spicules can explain the corona [Klimchuk, 2011]. Do they supply the corona with a majority of its hot plasma or is coronal heating and the associated evaporation of chromo-

spheric material still the dominant process? A related question is whether type II spicules are responsible for the bright emission that is observed from the lower transition region (LTR, $T \leq 0.1$ MK). Traditional models have difficulty explaining both the brightness of this emission and its rapid redshifts (although see *Hansteen et al.* [2010]). Henceforth, we use the shorthand “spicules” to refer to type II spicules.

It is important to distinguish between heating that occurs in the corona and heating that produces plasma at coronal temperatures. The two are not necessarily the same. We reserve the term “coronal heating” explicitly for energy deposition that takes place above the chromosphere (i.e., in plasmas that begin with temperatures $> 10^4$ K). The heating that raises the temperature of cold spicule material to coronal values is not included in this definition. Thus, we wish to know whether the corona is due to coronal heating or to spicules. Both play a role, but which dominates?

Although the physical origin of spicules has not yet been determined, it would seem that the evolution after they are formed can be reasonably well described by one-dimensional hydrodynamics. Spicules are highly columnated structures that expand upward along their primary axis. Almost certainly they are aligned with the magnetic field. If the field is untwisted, then the Lorentz force vanishes along the axis, and a non-magnetic driver is implied. Propagating twist could exert an upward magnetic force via the barber pole effect, but it is more likely that the spicule plasma is ejected along the field by a locally enhanced gas pressure at the base. Such a high pressure region would be produced, for example, when a reconnection outflow jet decelerates and its kinetic energy is thermalized. It could be also be produced by a squeezing of the flux tube from the interaction with emerging flux [*Martínez-Sykora, Hansteen, and Moreno-Insertis*, 2011].

This paper does not concern the origin of spicules, but rather what happens to the cool plasma as it is ejected. Observations show that most of it is heated rapidly to approximately 0.1 MK and falls back to the solar surface. A small fraction, usually at the tip, is heated to much higher temperatures and continues to rise into the corona. Our analysis begins just after this rapid heating occurs. The approach we take is to assume that all of the hot plasma in the corona comes from spicules and to consider the observational consequences of this assumption. We will show that predicted observations are in gross disagreement with actual observations, and conclude from this that the *a priori* assumption must be incorrect: spicules provide only a small fraction of the hot plasma that exists in the corona. Our analysis also leads us to suggest that most of the bright emission from the LTR comes from the bulk of the spicule material that is heated only to 0.1 MK or less.

Although our analytical treatment is highly simplistic, it captures the essential physics of the spicule phenomenon as it is currently understood based on available observations. Our conclusions must nonetheless be judged relative to the simplifying assumptions that we make. Hydrodynamic and MHD simulations as well as new observations will ultimately test the validity of these assumptions. What we offer here is a reasonable and we believe very meaningful early attempt at addressing this important problem. We note that parts of our analysis resemble the approach of *De Pontieu et al.* [2009].

Before proceeding to describe our model, we first discuss the differences between spicules and chromospheric evaporation. Some readers may wonder whether they are essentially the same thing. In fact, they are fundamentally different. Chromospheric evaporation is the response of the lower atmosphere to an increase in the downward thermal conduction

flux from the corona, as occurs when there is an increase in the coronal heating rate. Because the transition region is unable to radiate the extra energy, super-hydrostatic pressure gradients develop, and plasma is driven upward. If the heating remains steady, evaporation continues until there is an eventual balance among radiation, heating, and conduction. This is a static equilibrium. If the heating switches off, as in a nanoflare, the evaporated plasma cools and slowly drains back to the surface (e.g., *Klimchuk* [2006]; *Reale* [2010]).

A key point that is not generally appreciated is that the plasma at all temperatures in the transition region is heated by the thermal conduction flux during “chromospheric” evaporation. A common misconception is that the flux passes through the transition region and is deposited in the chromosphere below. In reality, only a very small fraction makes it to the chromosphere. Most of the energy is used up heating the transition region. It is helpful to think of the transition region as a stack of thin layers of different temperature. During evaporation, each layer is heated to progressively higher temperatures until they eventually become coronal. We have pointed out that spicules are likely driven upward by a localized pressure enhancement at their base. If that enhancement were due to a conduction flux from the corona, the flux would need to pass through not only the transition region, but also the cold plasma column that becomes the spicule. Clearly this is not possible, since the flux is proportional to $T^{5/2}\nabla T$, and both the temperature and temperature gradient are small in a spicule. A beam of high-energy particles could potentially deposit a large amount energy deep in the chromosphere, but flare simulations to date have not produced anything that resembles a spicule [*Fisher*, 2012; *Allred*, 2012].

It is also worth noting that the evaporation associated with coronal nanoflares is accompanied by a behavior that is exactly the opposite to what is observed in spicules. The 1 MK emission from spicules is observed to rise upward together with the cool jet when viewed near the limb [*De Pontieu et al.*, 2011]. In nanoflares, the 1 MK emission comes from the transition region footpoints of super-heated loop strands. The greatly increased pressure in these strands pushes the transition region and chromosphere downward, so the 1 MK emission layer is actually displaced deeper in the atmosphere by several thousand kilometers, even as the plasma itself is rapidly flowing upward from evaporation (Appendix A). It is clear that spicules are not manifestations of coronal nanoflares.

2. Model

As described in *De Pontieu et al.* [2011], most type II spicules are observed to evolve in a manner shown schematically in Figure 1. Ca II H (3968 Å) movies from the Solar Optical Telescope (SOT) on Hinode reveal a thin (diameter $d \approx 200$ km) jet of cool material ($T \approx 10^4$ K) extending upward from the limb at an apparent velocity $v \approx 100$ km s⁻¹ (blue). The disk counterparts are believed to be rapid blueshift events (RBEs) seen in H α [*Rouppé van der Voort et al.*, 2009]. Most of the material then disappears in Ca II and H α as it is heated to approximately 8×10^4 K and becomes visible in He II (304 Å) observations from the Atmospheric Imaging Assembly (AIA) on the Solar Dynamics Observatory (SDO) (green). Some of the material at the top (the upper fraction $\delta \approx 10\%$ by length) is heated to much higher temperatures of approximately 1-2 MK and is visible in the 171, 193, and 211 channels of AIA, which are dominated by Fe IX, Fe XII, and Fe XIV, respectively (red). The warm He II spicule falls back to the surface after reaching a maximum height $h_s \approx 10,000$ km, somewhat higher than that of the cool Ca II spicule

from which it is transformed. The hot material continues to rise rapidly upward into the corona and fades from view. (The dark red in the figure indicates temperature, not brightness.) Note that the actual length-to-diameter aspect ratio is a factor of 10 greater than indicated in the figure.

The simple model that we consider here examines the hydrodynamic evolution of the plug of hot (2 MK) plasma that appears abruptly at the top of the spicule. It is presumably much denser and possibly also much hotter than the ambient coronal plasma in the flux tube, so it should expand rapidly upward into the lower pressure region above. The fourth state in Figure 1 represents this expansion and eventual filling of the loop strand. Because we are testing the hypothesis that spicules explain the corona, the temperature must remain near 2 MK as the strand fills (Appendix B). The question of adiabatic cooling during the expansion is taken up later. If there is no coronal heating, the plasma will subsequently cool by radiation and thermal conduction and drain back down to the chromosphere. This is represented in the fifth state. Eventually the strand will become “empty” to match the initial conditions before the event occurred.

The sequence of events described above, with hot emission appearing near the top of the warm He II spicule, is most common, and we refer to it as Scenario A. A minority of spicules have a slightly different behavior in which the hot emission appears along the full length of the warm structure [*De Pontieu et al.*, 2011; *McIntosh*, 2011]. For these, we envision the configuration shown in Figure 2. The spicule contains spatially unresolved strands, most of which are near 8×10^4 K and some of which are near 2 MK. In this case the parameter $\delta \approx 1$ since the hot plasma occupies the full length of the spicule. The expansion of the plasma and subsequent cooling and draining are the same as before. We

call this Scenario B. Note that there is likely to be unresolved substructure in Scenario A as well. The figures are conceptual idealizations.

2.1. Blue Wing to Line Core Intensity Ratio

If a substantial amount of hot spicule material flows into the corona at speeds of approximately 100 km s^{-1} , then we should see evidence for it in the blue wings of spectral lines such as Fe XIV (274 \AA) when observed on the disk. Such evidence has been reported as red-blue (RB) asymmetries in the line profile by *Hara et al.* [2008]; *De Pontieu et al.* [2009]; *McIntosh and De Pontieu* [2009]; *De Pontieu et al.* [2011], and *Tian et al.* [2011]. These studies find that the excess intensity in the blue wing is approximately 5% of the intensity in the line core. *Doschek* [2012] reports intensity ratios of generally $< 5\%$ in Fe XII (195 \AA). Other researchers have had difficulty finding any detectable RB asymmetry.

The blue wing to line core intensity ratio provides an important constraint on the amount of coronal plasma that comes from spicules. Under our *a priori* assumption that all coronal plasma comes from spicules, we have a simple interpretation for both the wing and core emission. The wing emission is produced by the hot spicule material as it is rapidly expanding upward, and the core emission is produced by the same material as it cooling and slowly draining (the line core should be weakly redshifted). Of course we do not observe rising and falling material from the same event at the same time. Spicules are very small features, however, and there may be several unresolved events contributing to an observed line profile. Typical EUV spectrometer observations have an effective spatial resolution of 1 Mm or more, depending on pixel summing, and exposure times of several tens of seconds. If spicules occur randomly, then an observed line profile can be approximated by the time-averaged emission from a single event that has gone through a

complete upflow and downflow cycle. To predict the blue wing to line core intensity ratio, we must estimate the time-integrated emission separately for the upflow and downflow. We begin with the upflow.

Let $h_0 = \delta h_s$ be the length along the tube (vertical thickness) of the hot spicule material just after being heated to 2 MK. This heating occurs very rapidly based on the observation that Ca II spicules disappear from view in only 5-20 s [*De Pontieu et al.*, 2007]. Let n_0 be the electron number density at this time. Since mass is conserved as the hot material expands,

$$n(t)h(t) = n_0h_0. \quad (1)$$

For a constant expansion velocity, v ,

$$h(t) = h_0 + vt. \quad (2)$$

If we assume that the temperature remains near 2 MK during the expansion, as must be the case in order to explain coronal observations (see Appendix B), then the intensity of a given emission line is proportional to the column emission measure, n^2h . Substituting from above, we have

$$EM(t) = EM_0 \frac{1}{1 + vt/h_0}, \quad (3)$$

where $EM_0 = n_0^2h_0$ is the initial value. The time-integrated emission measure of the expanding hot plasma column at time t is therefore

$$EM^*(t) = \int_0^t EM(t)dt = EM_0 \frac{h_0}{v} \ln \left(1 + \frac{vt}{h_0} \right). \quad (4)$$

A typical coronal scale height $h_c = 5 \times 10^9$ cm is filled in upflow time $\tau_u = h_c/v = 500$ s. We take this to be the end of the expansion phase, so the time-integrated emission

measure of the upflow is

$$EM_u^* = EM^*(\tau_u) = \tau_u EM_0 f(x), \quad (5)$$

where $x = h_c/h_0$ and $f(x) = (1/x) \ln(1+x)$. As shown in Figure 3, $f(x) \approx 0.1$ for the reasonable range $0.05 \leq \delta \leq 0.3$, corresponding to $17 \leq x \leq 100$. Recall that $\delta = h_0/h_s$ is the fraction of the spicule that is heated to coronal temperatures. The time-integrated emission measure of the upflow is then

$$EM_u^* \approx 0.1 \tau_u n_0^2 \delta h_s. \quad (6)$$

The coefficient in the expression becomes 0.4 for scenario B, where $\delta = 1.0$.

After filling the loop strand, the plasma cools and drains. To explain the corona, its density must equal the characteristic density of the observed corona, n_c . We can write the emission measure as $n_c^2 h_c A$, where an area factor A is introduced to account for the difference in the average cross-sectional areas of the upflow and downflow. The magnetic field does not change between the upflow and downflow, but the integrated emission from the upflow is dominated by the earliest times, when the material is still low in the corona, whereas the emission from the downflow comes more or less uniformly from the full length of the strand. If the strand expands with height, then $A > 1$. *De Pontieu et al.* [2009] and *De Pontieu et al.* [2011] suggest $A = 3$, which seems reasonable. We note that both the upflow and downflow are well above the throat of rapid magnetic expansion at the base of the strand that is associated with the sharp transition from high to low plasma β .

The downflowing plasma will be visible in a line like Fe XIV (274 Å) only for a characteristic cooling time, τ_{cool} . This is true whether the cooling plasma begins near 2 MK, as we argue in Appendix B, or a higher temperature. The time-integrated emission measure

is therefore

$$EM_d^* = \tau_{cool} n_c^2 h_c A. \quad (7)$$

If we assume cooling by radiation and use the optically thin radiative loss function at 2 MK in *Klimchuk, Patsourakos, and Cargill* [2008], we have

$$\tau_{cool} < \tau_{rad} = 6.6 \times 10^{12} / n_c. \quad (8)$$

The inequality accounts for the fact that we have ignored cooling from thermal conduction and enthalpy, which can be significant [*Bradshaw and Cargill*, 2010]. The time-integrated emission measure of the downflow is finally

$$EM_d^* < 6.6 \times 10^{12} n_c h_c A. \quad (9)$$

The least known quantity in our analysis is the initial density of the hot plasma when it first appears at the tip of the spicule, n_0 . It can be eliminated from equation (6) using conservation of mass:

$$n_0 \delta h_s = n_c h_c A. \quad (10)$$

A typical coronal density of $n_c = 10^9 \text{ cm}^{-3}$ implies an initial density in the range $5 \times 10^{10} \leq n_0 \leq 3 \times 10^{11} \text{ cm}^{-3}$ for $0.3 \geq \delta \geq 0.05$. This compares favorably with the 10^{11} cm^{-3} density that is measured in ordinary spicules [*Beckers*, 1972; *Sterling*, 2000]. We can infer a lower limit for the density of type II spicules from the fact that they are seen as dark absorbing features in the AIA 171 channel before they are seen in emission [*De Pontieu et al.*, 2011]. An optical depth of unity resulting from continuum absorption at 171 Å requires either a hydrogen density of 10^{12} cm^{-3} or a helium density of $7 \times 10^{10} \text{ cm}^{-3}$, where we have assumed a spicule diameter of 200 km and absorption cross sections of 5×10^{-20}

cm² for H and 7×10^{-19} cm² for He [Chantler, 1995]. If the absorption were due only to H or only to He, and if the atoms were to become fully ionized during the sudden heating, the electron density at the time of initial 171 Å emission would be 10^{12} cm⁻³ or 1.4×10^{11} cm⁻³, respectively. This suggests that 10^{11} cm⁻³ is a reasonable lower limit for n_0 . We stress that our results below do not depend on n_0 . However, conservation of mass requires that n_0 be comparable to our estimates here if spicules are to explain the observed characteristic coronal density. Direct measurements of n_0 using the blue wing emission in density sensitive line pairs would provide a useful observational test, which we are currently pursuing [Patsourakos, Klimchuk, and Young, 2012]. A major discrepancy would indicate that a majority of coronal plasma cannot come from spicules.

Combining equations (6), (9), and (10), and using $\tau_u = h_c/v$, we obtain an expression for the ratio of the time-integrated emission measures of the upflow and downflow under scenario A:

$$R = \frac{EM_u^*}{EM_d^*} > 1.5 \times 10^{-14} \frac{n_c h_c^2 A}{\delta h_s v}. \quad (11)$$

This is the expected ratio of the blue wing to line core intensities of a hot coronal line like Fe XIV (274 Å). The only difference under scenario B is that the coefficient becomes 6×10^{-14} . Table 1 gives the predicted ratios for parameter values $h_c = 5 \times 10^9$ cm, $A = 3$, $h_s = 10^9$ cm, $v = 10^7$ cm s⁻¹, $\delta = 0.1$ (scenario A) or 1 (scenario B), and $n_c = 3 \times 10^9$ cm⁻³ (active region) or 10^9 cm⁻³ (quiet Sun). The coronal densities are those measured at 1-2 MK by Dere [1982], Doschek et al. [2007], and Young et al. [2009] in active regions, and by Feldman et al. [1978], Laming et al. [1997], and Warren and Brooks [2009] in the quiet Sun. We see that the predicted ratios are one to two orders of magnitude larger than the observed ratio, $R_{obs} \leq 0.05$. For scenario A, which is the better description of

most spicules, the predicted ratio exceeds the observed one by at least a factor of 68 in active regions and 22 in the quiet Sun. The disagreement is smallest for scenario B in the quiet Sun, where the difference is a factor of 9.

There is considerable uncertainty in the predicted ratios. If we allow each of the six parameters in equation (11) to be uncertain by a factor of 2, and if we assume that the errors are uncorrelated, then the combined uncertainty in R is a factor of 3.6. This is much too small to account for the discrepancy with observations. If we allow the parameters to be uncertain by a factor of 4, which seems excessive, then the uncertainty in R is a factor of 9, still too small, with the possible exception of scenario B in the quiet Sun.

A potential source of error is the assumption that all of the upflowing plasma is at temperatures where the emission line is sensitive. If this is not the case, so that a substantial portion of the upflow is invisible, then the predicted R must be adjusted downward. We argue in Appendix B that the range of temperatures in the upflow cannot be too broad if the corona is dominated by spicules, and therefore the correction to R should be modest. It is nonetheless important to determine the total emission measure of the upflow by measuring a differential emission measure distribution using the blue wing intensities of multiple spectral lines. We are currently undertaking such a study [*Tripathi et al.*, 2012].

The velocity of 10^7 cm s⁻¹ that we have used in equation (11) is based in large degree on the Doppler shift of EUV blue wing emission observed near disk center (and also on proper motions observed near the limb). If the coronal strand is inclined relative to vertical, the actual velocity will be larger than the Doppler shift. Equation (11) still applies, however, because the length of the strand must be increased by an equal factor in order for its vertical extent to remain h_c . Our substitution $\tau_u = h_c/v$ is independent of the strand

inclination if v is the Doppler shift. We note that the expansion of the hot plasma could be as fast as the sound speed, which is $2.3 \times 10^7 \text{ cm s}^{-1}$ at $T = 2 \text{ MK}$.

Even taking these factors into account, there remains a large discrepancy between the predicted and observed values of R , and this suggests that only a small fraction of the hot plasma in the corona can come from spicules. It is straightforward to show that the ratio of spicule to non-spicule emission measures is given by $f_s = R_{obs}/R$. Values of f_s based on Table 1 are presented in Table 2. Spicules appear to account for less than 1.4% of the coronal plasma in active regions under scenario A. They could account for as much as 11% of the coronal plasma in the quiet Sun under scenario B, but we must remember that scenario B is believed to be relatively uncommon. Note that the predicted R given in equation (11) uses the characteristic observed coronal density, n_c . If spicules play only a small role in the corona, then their density could be much different, and f_s may not be accurate. Of course it cannot approach unity, because then the spicule density must be close to the characteristic density, and we know that this gives an f_s that is very small.

2.2. Adiabatic Cooling

Let us suppose for the moment that the above analysis is somehow invalid and that spicules do in fact provide most of the observed coronal mass. There is still the need for substantial heating well above the chromosphere. In the absence of such coronal heating, the expanding plasma would cool by radiation, thermal conduction, and especially by the work it performs during the expansion. Adiabatic expansion alone is enough to decrease the temperature dramatically. In order to end with a characteristic coronal temperature of 2 MK when the strand is filled, the upflowing plasma would need to begin at a much higher temperature: 58 MK in scenario A and 13 MK in scenario B. This can be ruled

out because the emission at these temperatures would be much brighter than observed, as discussed in Appendix B.

For adiabatic expansion, PV^γ is a constant, where V is the volume of the expanding column and $\gamma = 5/3$ is the ratio of specific heats. It is easy to show that an initial temperature T_0 leads to a final temperature

$$T_c = \left(\frac{\delta h_s}{h_c A} \right)^{2/3} T_0. \quad (12)$$

For $T_0 = 2$ MK, the final temperature is 7×10^4 K in scenario A and 3×10^5 K in scenario B. Thus, it requires essentially as much energy to maintain the plasma at 2 MK as it does to produce it in the first place. This heating must occur throughout the corona.

2.3. Lower Transition Region (LTR) Emission

As indicated in Figure 1, only the top fraction δ of the cool spicule gets heated to coronal temperatures in scenario A. Most of the rest gets heated to around 10^5 K and is visible in He II (304 Å) for $\tau_{LTR} \approx 300$ s as it falls back to the surface [De Pontieu *et al.*, 2011]. Its time-integrated emission measure is given by

$$EM_{LTR}^* = \tau_{LTR}(1 - \delta)n_0^2 h_s, \quad (13)$$

where we have assumed that its density is the same as the initial density of the hot material, n_0 . We can compare this with the time-integrated emission measure of the downflowing coronal plasma near 2 MK, EM_d^* , given by equation (9). Using conservation of mass, equation (10), we obtain the ratio

$$\frac{EM_{LTR}^*}{EM_d^*} > 1.5 \times 10^{-13} \frac{1 - \delta}{\delta^2} \frac{h_c}{h_s} A n_c \tau_{LTR}. \quad (14)$$

The actual ratio is likely to significantly exceed the lower limit for several reasons. First, equation (9) is a lower limit because cooling from thermal conduction and enthalpy are

ignored. Second, the average density of the spicule may be greater than the density of the top part that gets heated to 2 MK. Third, the spicule material may continue to radiate after it has fallen back to the surface and is no longer visible in He II at the limb (i.e., the lifetime may be longer than 300 s). Finally, equation (14) does not include LTR emission coming from the conventional transition region at the base of the strand that is powered by the thermal conduction and enthalpy fluxes from the cooling coronal plasma. Table 3 gives the predicted ratios for $h_c = 5 \times 10^9$ cm, $h_s = 10^9$ cm, $A = 3$, $n_c = 3 \times 10^9$ cm $^{-3}$, $\tau_{LTR} = 300$ s, and several different values for δ . The ratios range from 16 to 770.

Let us assume for the moment that all of the plasma that does not reach coronal temperatures (the green material in Figure 1) is heated to the temperature range centered on $T = 0.08$ MK where He II (304 Å) is sensitive. This range has an approximate width $\Delta \log T = 0.3$, as does the temperature range of the coronal line used to determine EM_d^* (see below). Under this assumption, the ratio of the emission measures in equation (14) is approximately equal to the ratio of $T \times DEM(T)$ evaluated at 0.08 MK and 2 MK. Using the differential emission measure distributions of *Raymond and Foukal* [1981]; *Raymond and Doyle* [1982]; *Dere and Mason* [1993], and *Landi and Chiuderi Drago* [2009], we obtain observed ratios less than 0.1, as indicated in the third column of the table. The ratios are especially small in active regions.

Most of the spicule material is heated above 0.02 MK, since the spicule disappears in Ca II, but some of it may not be heated enough to be visible in He II. To allow for this possibility, we have integrated $DEM(T)$ from the above cited papers between 0.02 and 0.1 MK to obtain an alternative estimate for EM_{LTR}^* . For the coronal plasma we use

$$EM_d^* = \ln 10 T DEM \Delta \log T \quad (15)$$

evaluated at 2 MK with $\Delta \log T = 0.3$. This is approximately equivalent to integrating $DEM(T)$ over a temperature interval corresponding to a temperature decrease of a factor of 2, as would occur during a coronal cooling time. The observed emission measure ratio obtained in this way is less than 3 (< 1 in active regions), as indicated in the last column of Table 3. Though smaller, there remains a major discrepancy between the predicted and observed ratios. This leads us to once again conclude that our *a priori* assumption is incorrect, and spicules can account for only a minor fraction of the hot plasma in the corona.

Although it would seem that spicules are not important for the corona in a global sense, they may be extremely important in the loop strands in which they occur. Furthermore, we suggest that spicules play a dominant role globally in producing the majority of the $2 \times 10^4 \leq T \leq 10^5$ K emission from the Sun. The lower transition region in standard coronal heating models is much too faint at these temperatures. The models predict that $DEM(T)$ should decrease with decreasing temperature throughout the transition region, but observations show a sharp upturn as the temperature drops below about 0.1 MK. This is true whether the heating is steady or impulsive. Small low-lying loops that are everywhere cooler than 0.1 MK might explain the excess emission in mixed polarity regions of the quiet Sun [*Antiochos and Noci, 1986*], but these cool loops will not be present in the large unipolar areas of active regions. Spicules very likely provide the excess emission below 0.1 MK in these regions.

Spicules may also explain the rather strong redshifts of 10-15 km s⁻¹ that are observed in the LTR of the quiet Sun [*Peter and Judge, 1999*] and active regions [*Klimchuk, 1987*]. If the material seen in He II (304 Å) falls at even a fraction of its upflow speed, then

large redshifts are possible. Parabolic trajectories seen in height-time plots from limb observations in He II support this conjecture [De Pontieu *et al.*, 2011]. We note that Hansteen *et al.* [2010] have offered a different explanation for the redshifts. Redshifts are also expected from cooling and draining after coronal nanoflares, but whether the speeds are sufficiently large is currently being investigated [Reep, Bradshaw, and Klimchuk, 2012].

2.4. High-Frequency Spicules

De Pontieu *et al.* [2011] have proposed a spicule scenario that is significantly different from the two scenarios we have discussed so far. Call it scenario C. A given coronal strand may experience multiple spicule ejections. The frequency of events in scenarios A and B is low in the sense that the coronal plasma from one spicule has time to cool and drain before the next spicule occurs. For typical coronal densities, the cooling time given by equation (8) is roughly 2000 s in active regions and 7000 s in the quiet Sun. Spicules are proposed to occur much more frequently in scenario C. Based on disk observations of H_{α} rapid blueshift events (RBEs), De Pontieu *et al.* [2011] suggest that the recurrence time at the same location may be as short as 500 s. Using conservative estimates for the density of the ejected hot plasma, they conclude that each event contributes only a few percent of the material in a typical coronal strand. Presumably the mass slowly builds up until coronal densities are reached, at which point continued ejections offset the mass loss from draining. De Pontieu *et al.* estimate that the flux of kinetic and thermal energy in the spicules is adequate to sustain the radiative and conductive energy losses from the strand once it is fully developed.

We find two significant difficulties with this scenario. The first concerns the evolution of the loop strand. If each spicule contributes a few percent of the eventual mass, then

at least 20 spicules are required to reach the final state (more if any draining takes place during the buildup). At a frequency of one per 500 s, approximately 10^5 s are required for a fully developed strand to appear. In contrast, 1-2 MK coronal loops are observed to brighten and fade over a total lifetime of only 1000-5000 s [*Klimchuk, Karpen, and Antiochos, 2010*]. Scenario C would seem to be incapable of explaining such loops. This argument does not, however, rule out scenario C as a possible explanation for the diffuse corona. Even loops might be explained if the actual density of the ejected hot plasma is much larger than the value assumed. In that case fewer spicules, and less time, would be needed to create the strand. A potential problem is that the bigger ejections might produce brightness fluctuations larger than observed [*De Pontieu et al., 2011*].

Perhaps a greater concern about scenario C is whether it can explain the temperature structure of the corona. The maximum temperature is observed to occur near the strand apex, not near the footpoints. Each spicule under scenario C provides hot plasma and energy only to the extreme lower part of the strand, since the newly ejected plasma cannot pass through the pre-existing plasma from the earlier ejections. An upwardly directed thermal conduction flux is therefore required to power the radiation from the overlying material. This implies a temperature inversion, with the maximum temperature occurring near the base. It can be shown that the temperature scale height needed to carry this conduction flux is approximately 1.7×10^9 cm in active regions and 5.1×10^9 cm in the quiet Sun. This can be easily ruled out observationally. Waves may be generated during the spicule ejections, and these might heat the corona and eliminate the need for a temperature inversion, but this would constitute coronal heating [*McIntosh et al., 2011*].

3. Conclusions

The discovery of type II spicules and their association with red-blue asymmetries in EUV spectral lines suggested the interesting possibility that most coronal plasma comes from spicule material that is heated to ≈ 2 MK as it is ejected. The need for coronal heating—energy deposition in the corona itself—was brought into question. We have presented a very simple yet physically meaningful model that seems to rule out this possibility. According to our calculations, spicules provide only a small fraction of the hot plasma that exists in the corona ($< 2\%$ in active regions and $< 5\%$ in the quiet Sun). The large majority of coronal plasma comes from chromospheric evaporation, a fundamentally different process that results from coronal heating. Furthermore, even if the coronal plasma were to originate in spicules, coronal heating would still be required to maintain the hot temperature as the material expands. The need for energy release in the corona is unavoidable.

Our approach has been to assume that all coronal plasma comes from spicules and then to examine the observational consequences. One consequence is that the red-blue asymmetry of spectral lines, which relates to the excess intensity in the blue wing relative to the line core, would be many times larger than observed. The discrepancy is roughly two orders of magnitude in active regions. Another consequence is that the ratio of emission measures in the lower transition region and corona would be much too large, again by about two orders of magnitude. These comparisons must be judged against the simplicity of the model and the assumptions inherent to it. More sophisticated hydrodynamic and MHD simulations must be performed for verification (e.g., *Sterling, Shibata, and Mariaka*

[1993]; *Martínez-Sykora et al.* [2011]; *Judge et al.* [2012]). Nonetheless, the enormity of the discrepancies suggests that the basic conclusions are correct.

While it seems that spicules play only a minor role in supplying hot plasma to the corona, they may be extremely important for understanding the lower transition region. Standard models based on coronal heating predict far too little emission from the LTR, whereas spicules should be very bright at these temperatures. We are led to the following picture. The upper solar atmosphere (transition region and corona) is filled with thin magnetic flux tubes that are at or below the resolving capability of our best instruments. Most are populated with plasma as a consequence of coronal heating, the precise altitude of this heating not yet established. Interspersed among them are much fewer flux tubes that experience type II spicule ejections. The part of the spicule that is heated to high temperatures expands into the corona and produces strongly blue-shifted emission at EUV wavelengths. Because the emission is much fainter than the emission from all the other flux tubes, it appears as only a weak enhancement in the blue wing of spatially unresolved line profiles. Blue wing emission is also produced by chromospheric evaporation that accompanies coronal nanoflares, but it is expected only in lines hotter than 2 MK [*Patsourakos and Klimchuk*, 2006]. The bulk of the spicule mass is heated to ≤ 0.1 MK and emits strongly as it falls back to the surface. Thus, a majority of LTR plasma is contained in spicule flux tubes, and a majority of coronal plasma is contained in non-spicule flux tubes.

There is still much to learn about type II spicules, including how they are created in the first place. Our analysis here has examined only what happens after they are formed. One interesting question is whether spicules are different in mixed magnetic polarity

areas of the quiet Sun and unipolar areas of active regions and coronal holes. Magnetic reconnection in mixed polarities can involve oppositely directed fields (e.g., between a long flux strand and a small “magnetic carpet” loop), but only “component reconnection” is possible where the field is unipolar. Is this an important difference? Initial reports were that type II spicules are generally similar everywhere on the Sun: active regions, quiet Sun, and coronal holes. If true, this would be further evidence that spicules do not provide most of the coronal plasma, since the properties of the corona are much different in these different regions. On the other hand, the properties of the LTR are also different, and if the LTR is due primarily to spicules, one might expect the spicules to be different too. New observations from the upcoming Interface Region Imaging Spectrograph (IRIS) mission, combined with detailed modeling, will help us to answer these and other crucial questions concerning this fascinating phenomenon.

Appendix A: Proper Motion of 1 MK Emission During Coronal Nanoflares

We here demonstrate that the proper motion of 1 MK emission is expected to be downward in the case of a coronal nanoflare, opposite to what is observed in spicules. We present the results of two simulations performed with the ARGOS 1D hydrodynamics code [*Antiochos et al.*, 1999]. In both simulations we begin with a semi-circular coronal loop strand of 7.5×10^9 cm halflength that is maintained in a static equilibrium by a uniform 10^{-6} erg cm $^{-3}$ s $^{-1}$ volumetric heating rate. Chromospheric sections with many scale heights of 3×10^4 K plasma are attached at each end. In the first simulation, we set off an impulsive nanoflare corresponding to a rapid increase and decrease in the spatially uniform heating rate. The temporal profile is triangular and lasts a total of 50 s. The total energy input is 5.625×10^9 ergs. This simulation is identical to Example 2 in *Klimchuk*,

Patsourakos, and Cargill [2008] except that heat flux saturation is included in the present case.

Figure A1 shows synthetic observations corresponding to the 171 channel of the Transition Region and Coronal Explorer (TRACE). The bandpass is similar to the 171 channel of SDO and is dominated by lines of Fe IX and X, formed near 1 MK. Intensity is plotted as a function of position near the “left” footpoint of the loop (the apex is located at $s = 135$ Mm). The black, green, red, and blue curves correspond to 30, 60, 90, and 120 s after the start of the nanoflare, respectively. We see that the 171 emission feature moves downward with a maximum velocity of about 100 km s^{-1} . It lasts for approximately one minute, at which point the intensity and velocity decrease dramatically. A period of slow ($< 15 \text{ km s}^{-1}$) and very faint (normalized intensity $< 1\%$) upward motion follows.

The second example considers a more gradual nanoflare. The total energy release is the same, but it is now spread out over 500 s. This is the same simulation as Example 1 in *Klimchuk, Patsourakos, and Cargill* [2008] and discussed in *Klimchuk* [2006] (the case without saturated heat flux). Figure A2 shows the 171 intensity profiles at 100, 200, 300, and 400 s after the start of the nanoflare. Again, the proper motion of the emission layer is initially downward, this time peaking at about 30 km s^{-1} . The subsequent upward displacement is perhaps bright enough to be detected, but it is much slower ($< 5 \text{ km s}^{-1}$) than observed in spicules. It is clear that spicules are not produced by coronal nanoflares. The proper motion of hot emission is wrong, and more importantly, there is no ejection of plasma at chromospheric temperatures.

Appendix B: Constant Temperature Upflow

We show here that, in order for spicules to explain the corona, the hot plasma must maintain a roughly constant temperature of roughly 2 MK from the time it is first created to the time it has filled the loop strand and started to cool. First consider the possibility that the plasma at the tip begins at a much higher temperature ($T_0 > 10$ MK; Section 2.2) so that it cools adiabatically to the characteristic coronal value of 2 MK at the end of the expansion. How bright would this plasma be? From equation (12), the height of the expanding column at the time when the temperature has dropped by a factor of two is

$$h = \frac{2^{3/2}\delta h_s}{A_h}, \quad (\text{B1})$$

where A_h is the average cross sectional area of the strand up to height h compared to the area at h_0 . Using equation (4) with $vt = h$ and $h_0 = \delta h_s$, we find that the time-integrated emission measure up to this point in the expansion is

$$EM_h^* = 0.7 \frac{h}{v} EM_0. \quad (\text{B2})$$

We have taken 0.7 for function $f(x) = f(h/h_0) = f(2^{3/2}/A_h)$, which actually ranges between 0.47 for $A_h = 1$ and 1.0 for $A_h = \infty$. Equations (B1) and (B2) together with equations (9) and (10) give

$$\frac{EM_h^*}{EM_d^*} > 3 \times 10^{-13} \frac{n_c h_c A}{v A_h}. \quad (\text{B3})$$

EM_h^* is the emission measure that would be inferred from a spectral line that is sensitive to the initial hot temperature T_0 . EM_d^* is the emission measure of the cooling downflow that would be inferred from a 2 MK emission line, such Fe XIV (274 Å). Recall that we used a cooling time appropriate to 2 MK in equation (8). For $n_c = 3 \times 10^9 \text{ cm}^{-3}$, $h_c = 5 \times 10^9 \text{ cm}$,

$v = 10^7 \text{ cm}^{-3} \text{ s}^{-1}$, $A = 3$ and $A_h = 1.5$, we have that $EM_h^* > 0.9EM_d^*$. The observationally derived emission measure of the super hot plasma at the start of adiabatic expansion is predicted to be comparable to or perhaps greater than the observationally derived emission measure at 2 MK. This contradicts actual observations, which show that emission measure distribution peaks near 2-3 MK and decreases steeply at higher temperatures [*Patsourakos and Klimchuk, 2009; Reale et al., 2009; Tripathi, Klimchuk, and Mason, 2011; Winebarger et al., 2011; Warren, Winebarger, and Brooks, 2012; Schmelz and Pathak, 2012*]. We conclude that spicules cannot be heated initially to much beyond 2 MK unless our *a priori* assumption is wrong and spicules account for only a small fraction of the plasma in the corona.

Now consider the possibility that the plasma ends the expansion phase and begins the cooling and draining phase at a temperature above 2 MK. *Sturrock et al. [1990]* demonstrated that the differential emission measure distribution of a radiatively cooling plasma is the inverse of the optically thin radiation loss function. Since the loss function is mostly a decreasing function of temperature above 0.1 MK (it has a weakly positive $T^{1/3}$ dependence between 4 and 8 MK; *Klimchuk, Patsourakos, and Cargill [2008]*), the DEM should be an increasing function of temperature, and therefore the peak DEM should occur at the temperature where the cooling begins. Observed DEM distributions peak near 2-3 MK, so this must be the temperature at the start of downflow and end of the expansion upflow. The same conclusion is reached if thermal conduction and enthalpy are included in the cooling [*Bradshaw, Klimchuk, and Reep, 2012*].

Thus, if the corona is due to spicules, the temperature of the hot material both at the start and end of expansion must be roughly 2 MK. As discussed in Section 2.2, as much

heating is required to maintain the temperature in the face of adiabatic expansion as is required to produce the hot plasma in the first place. This heating occurs in the corona.

Acknowledgments. This work was supported by the NASA Supporting Research and Technology Program. The author thanks many people for useful discussions, but especially Bart De Pontieu. Martin Laming, John Raymond, Scott McIntosh, and Nicholeen Viall were also particularly helpful.

References

- Allred, J. C., private communication.
- Antiochos, S. K., MacNeice, P. J., Spicer, D. S., and Klimchuk, J. A. (1999), The Dynamic Formation of Prominence Condensations, *Astrophys. J.*, *512*, 985–991.
- Antiochos, S. K., and Noci, G. (1986), The Structure of the Static Corona and Transition Region, *Astrophys. J.*, *301*, 440–447.
- Athay, R. G., and Holzer, T. E. (1982), The Role of Spicules in Heating the Solar Atmosphere, *Astrophys. J.*, *255*, 743–752.
- Beckers, J. M. (1972), Solar Spicules, *Ann. Rev. Astron. Astrophys.*, *10*, 73–100.
- Bradshaw, S. J., and Cargill, P. J. (2010), The Coolign of Coronal Plasmas. III. Enthalpy Transfer as a Mechanism for Energy Loss, *Astrophys. J.*, *717*, 163–174.
- Bradshaw, S. J., Klimchuk, J. A., and Reep, J. W. (2012), Diagnosing the Time-Dependence of Active Region Core Heating from the Emission Measure: I. Low-Frequency Nanoflares, *Astrophys. J.*, submitted.
- Chantler, C. T. (1995), Theoretical Form Factor, Attenuation and Scattering Tabulation for $Z=1-92$ from $E=1-10$ eV to $E=0.4-1.0$ MEV, *J. Phys. Chem. Ref. Data*, *24*, 71–643.

- Dere, K. P. (1982), Extreme Ultraviolet Spectra of Solar Active Regions and Their Analysis, *Solar Phys.*, *77*, 77–93.
- Dere, K. P., and Mason, H. E. (1993), Nonthermal Velocities in the Solar Transition Zone Observed With the High-Resolution Telescope and Spectrograph, *Solar Phys.*, *144*, 217–241.
- De Pontieu, B., et al. (2007), A Tale of Two Spicules: The Impact of Spicules on the Magnetic Chromosphere, *Pub. Ast. Soc. Japan*, *59*, S655–S662.
- De Pontieu, B., McIntosh, S. W., Hansteen, V. H., and Schrijver, C. J. (2009), Observing the Roots of Solar Coronal Heating—In the Chromosphere, *Astrophys. J.*, *701*, L1–L6.
- De Pontieu, B., et al. (2011), The Origins of Hot Plasma in the Solar Corona, *Science*, *331*, 55–58.
- Doschek, G. A. (2012), The Dynamics and Heating of Active Region Loops, *Astrophys. J.*, submitted.
- Doschek, G. A., et al. (2007), The Temperature and Density Structure of an Active Region Observed With the Extreme-Ultraviolet Imaging Spectrometer on Hinode, *Pub. Ast. Soc. Japan*, *59*, S707–S712.
- Feldman, U., Doschek, G. A., Mariska, J. T., Bhatia, A. K., and Mason, H. E. (1978), Electron Densities in the Solar Corona from Density-Sensitive Line Ratios in the N I Isoelectronic Sequence, *Astrophys. J.*, *226*, 674–678.
- Fisher, G. H. (2012), private communication.
- Hansteen, V. H., Hara, H., De Pontieu, B., & Carlsson, M. (2010), On Redshifts and Blueshifts in the Transition Region and Corona, *Astrophys. J.*, *718*, 1070–1078.

- Hara, H., et al. (2008), Coronal Plasma Motions Near Footpoints of Active Region Loops Revealed From Spectroscopic Observations With Hinode EIS, *Astrophys. J.*, 678, L67–L71.
- Judge, P. G., De Pontieu, B., McIntosh, S. W., and Olluri, K. (2012), The Connection of Type II Spicules to the Corona, *Astrophys. J.*, 746, 158–166.
- Klimchuk, J. A. (1987), On the Large-Scale Dynamics and Magnetic Structure of Solar Active Regions, *Astrophys. J.*, 323, 368–379.
- Klimchuk, J. A. (2006), On Solving the Coronal Heating Problem, *Solar Phys.*, 234, 41–77.
- Klimchuk, J. A. (2011), Are Spicules the Primary Source of Hot Coronal Plasma?, *Bull. Am. Astron. Soc.*, 43, #18.01.
- Klimchuk, J. A., Karpen, J. T., and Antiochos, S. K. (2010), Can Thermal Nonequilibrium Explain Coronal Loops?, *Astrophys. J.*, 714, 1239–1248.
- Klimchuk, J. A., Patsourakos, S., and Cargill, P. J. (2008), Highly Efficient Modeling of Dynamic Coronal Loops, *Astrophys. J.*, 682, 1351–1362.
- Laming, J. M., et al. (1997), Electron Density Diagnostics For the Solar Upper Atmosphere From Spectra Obtained By SUMER/SOHO, *Astrophys. J.*, 485, 911–919.
- Landi, E., and Chiuderi Drago, F. (2008), The Quiet-Sun Differential Emission Measure From Radio and UV Measurements, *Astrophys. J.*, 675, 1629–1636.
- Madjarska, M. S., Vanninathan, K., and Doyle, J. G. (2011), Can Coronal Hole Spicules Reach Coronal Temperatures?, *Astron. Astrophys.*, 532, L1–L4.
- Martínez-Sykora, J., De Pontieu, B., Hansteen, V. H., and McIntosh, S. W. (2011), What Do Spectral Line Profile Asymmetries Tell Us About the Solar Atmosphere?, *Astrophys. J.*, 732, 84–109.

- Martínez-Sykora, J., Hansteen, V., and Moreno-Insertis, F. (2011), On the Origin of the Type II Spicules: Dynamic Three-Dimensional MHD Simulations, *Astrophys. J.*, *736*, 9–20.
- McIntosh, S. W. (2011), private communication.
- McIntosh, S. W., and De Pontieu, B. (2009), High-Speed Transition Region and Coronal Upflows in the Quiet Sun, *Astrophys. J.*, *707*, 524–538.
- McIntosh, S. W., De Pontieu, B., Carlsson, M., Hansteen, V., Boerner, P., and Goossens, M. (2011), Alfvénic Waves with Sufficient Energy to Power the Quiet Solar Corona and Fast Solar Wind, *Nature*, *475*, 477–480.
- Patsourakos, S., and Klimchuk, J. A. (2006), Nonthermal Spectral Line Broadening and the Nanoflare Model, *Astrophys. J.*, *647*, 1452–1465.
- Patsourakos, S., and Klimchuk, J. A. (2009), Spectroscopic Observations of Hot Lines Constraining Coronal Heating in Solar Active Regions, *Astrophys. J.*, *696*, 760–765.
- Patsourakos, S., Klimchuk, J. A., and Young, P. R. (2012), in preparation.
- Peter, H., and Judge, P. G. (1999), On the Doppler Shifts of Solar Ultraviolet Emission Lines, *Astrophys. J.*, *522*, 1148–1166.
- Raymond, J. C., and Doyle, J. G. (1981), The Energy Balance in Coronal Holes and Average Quiet-Sun Regions, *Astrophys. J.*, *247*, 686–691.
- Raymond, J. C., and Foukal, P. (1982), The Thermal Structure of Coronal Loops and Implications for Physical Models of Coronae, *Astrophys. J.*, *253*, 323–329.
- Reale, F. (2010), Coronal Loops: Observations and Modeling of Confined Plasma, *Living Rev. Solar Phys.*, *7*, 5–78.

- Reale, F., Testa, P., Klimchuk, J. A., and Parenti, S. (2009), Evidence of Widespread Hot Plasma in Nonflaring Coronal Active Region From Hinode/X-Ray Telescope, *Astrophys. J.*, *698*, 756–765.
- Reep, J. W., Bradshaw, S. J., and Klimchuk, J. A. (2012), *Astrophys. J.*, in preparation.
- Roupe van der Voort, L., Leenaarts, J., De Pontieu, B., Carlsson, M., and Vissers, G. (2009), On-Disk Counterparts of Type II Spicules in the Ca II 854.2 nm and H α Lines, *Astrophys. J.*, *705*, 272–284.
- Schmelz, J. T., and Pathak, S. (2012), The Cold Shoulder: Emission Measure Distributions of Active Region Cores, *Astrophys. J.*, in press.
- Sterling, A. C. (2000), Solar Spicules: A Review of Recent Models and Targets for Future Observations, *Solar Phys.*, *196*, 79–111.
- Sterling, A. C., Shibata, K., and Mariska, J. T. (1993), Solar Chromospheric and Transition Region Response to Energy Deposition in the Middle and Upper Chromosphere, *Astrophys. J.*, *407*, 778–789.
- Sturrock, P. A., Dixon, W. W., Klimchuk, J. A., and Antiochos, S. K. (1990), Episodic Coronal Heating, *Astrophys. J.*, *356*, L31–L34.
- Tian, H., et al. (2011), Two Components of the Solar Coronal Emission Revealed by Extreme-Ultraviolet Spectroscopic Observations, *Astrophys. J.*, *738*, 18–27.
- Tripathi, D., Klimchuk, J. A., and Mason, H. E. (2011), Emission Measure Distribution and Heating of Two Active Region Cores, *Astrophys. J.*, *740*, 111–120.
- Tripathi, D., Klimchuk, J. A., Mason, H. E., and Young, P. R. (2011), in preparation.
- Warren, H. P., and Brooks, D. H. (2009), The Temperature and Density Structure of the Solar Corona. I. Observations of the Quiet Sun with the EUV Imaging Spectrometer

on Hinode, *Astrophys. J.*, 700, 762–773.

Warren, H. P., Winebarger, A. R., and Brooks, D. H. (2012), A Systematic Study of High Temperature Emission in Solar Active Regions, *Astrophys. J.*, in press.

Winebarger, A. R., Schmelz, J. T., Warren, H. P., Saar, S. H., and Kashyap, V. L. (2011), Using Differential Emission Measure and Density Measurements in an Active Region Core to Test a Steady Heating Model, *Astrophys. J.*, 740, 2 (12pp).

Young, P. R., Watanabe, T., Hara, H., and Mariska, J. T. (2009), High-Precision Density Measurements in the Solar Corona I. Analysis Methods and Results for Fe XII and Fe XIII, *Astron. Astrophys.*, 495, 587–606.

Xhang, Y. Z., Shibata, K., Wang, J. X., Mao, X. J., Matsumoto, T., Liu, Y., and Su, J. T. (2012), Revision of Solar Spicule Classification, *Astrophys. J.*, 750, 16–24.

Table 1. Blue Wing to Line Core Intensity Ratio, R

	Scenario A	Scenario B	Observed
Active Region	> 3.4	> 1.4	≤ 0.05
Quiet Sun	> 1.1	> 0.46	≤ 0.05

Table 2. Fraction of Hot Coronal Plasma Due to Spicules, f_s

	Scenario A	Scenario B
Active Region	$< 1.4\%$	$< 3.4\%$
Quiet Sun	$< 4.5\%$	$< 11\%$

Table 3. Lower Transition Region to Corona Emission Measure Ratio

δ	Predicted	Observed (He II 304)	Observed ($T \leq 0.1$ MK)
0.05	> 770	< 0.1	< 3
0.1	> 180	< 0.1	< 3
0.2	> 41	< 0.1	< 3
0.3	> 16	< 0.1	< 3

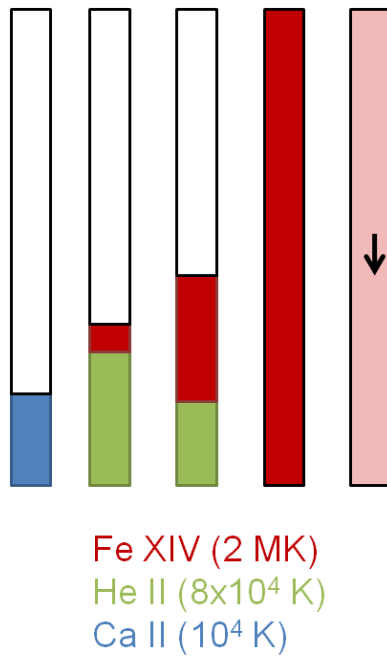


Figure 1. Schematic representation of the plasma evolution under type II spicule scenario A (most common). Time increases from left to right. 1. Rising spicule is visible in Ca II (3968 \AA) and H_{α} . 2. Most of the spicule is heated to < 0.1 MK (green) and becomes visible in He II (304 \AA) as it continues to rise; tip is heated to ~ 2 MK (red) and becomes visible in Fe XIV (274 \AA). 3. Warm material falls and hot material expands into the corona. 4. Loop strand becomes filled with hot material. 5. Material cools and drains slowly back to surface.

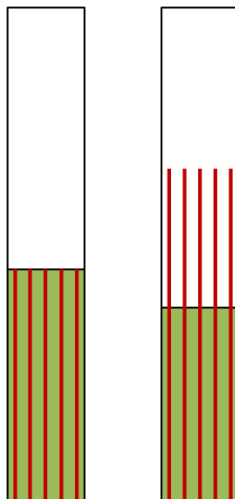


Figure 2. Schematic representation of the plasma evolution under type II spicule scenario B (least common). 1. Spatially unresolved warm (green) and hot (red) sub-strands appear together. 2. Warm material falls and hot material expands into the corona.

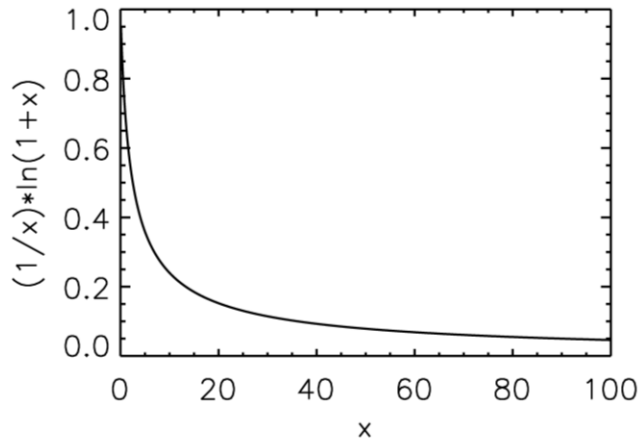


Figure 3. The function $f(x) = (1/x) \ln(1+x)$ used in equation (5).

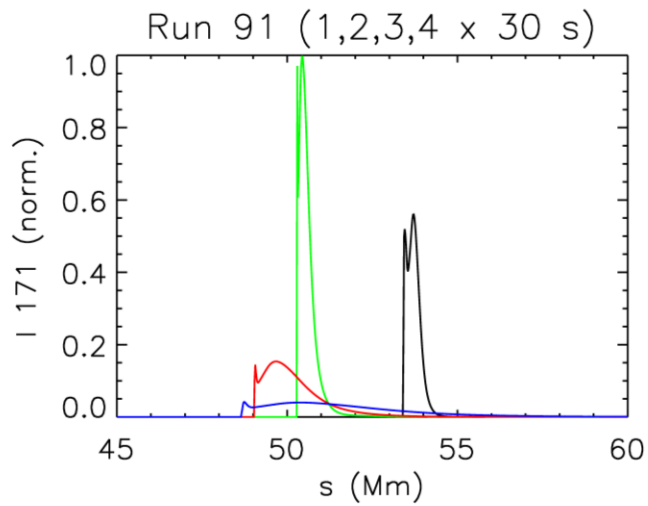


Figure A1. Simulated TRACE 171 observation of the footpoint region of a loop strand heated by a 50 s nanoflare. Shown are profiles of normalized intensity versus position at times of 30 (black), 60 (green), 90 (red), and 120 s (blue) after the start of the nanoflare. Increasing s corresponds to the upward direction.

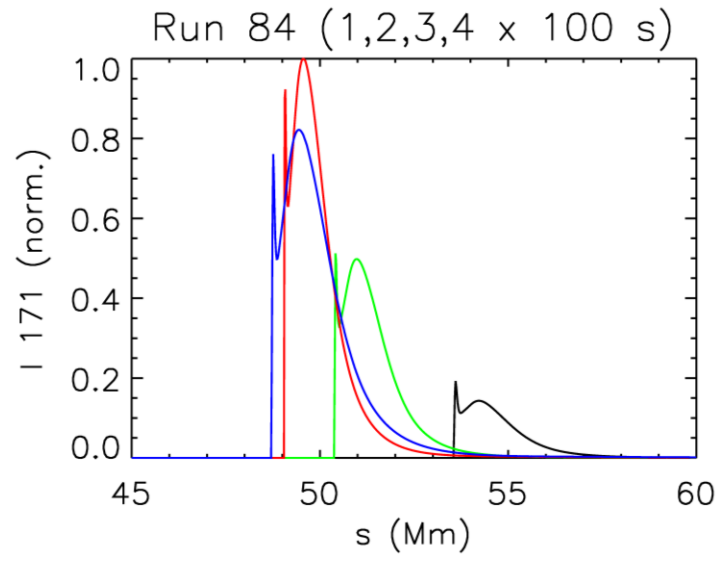


Figure A2. As in Figure A2 except for a 500 s nanoflare. Profiles are from 100 (black), 200 (green), 300 (red), and 400 s (blue) after the start of the nanoflare.